Portable Ultrasonic 3D Tag System Based On a Quick Calibration Method*

Akifumi Nishitani
Tokyo University of Science
2641, Yamazaki, Noda-shi, Chiba,
278-8510, Japan
a-nishitani@aist.go.jp

Yoshifumi Nishida
Digital Human Research Center, AIST
& CREST, JST
2-41-6, Aomi, Koto-ku, Tokyo,
135-0064, Japan
y.nishida@aist.go.jp

Toshio Hori
Digital Human Research Center, AIST
& CREST, JST
2-41-6, Aomi, Koto-ku, Tokyo,
135-0064, Japan
t.hori@aist.go.jp

Hiroshi Mizoguchi
Tokyo University of Science
2641, Yamazaki, Noda-shi, Chiba,
278-8510, Japan
hm@rs.noda.tus.ac.jp

Abstract – *The ability to quickly construct a human activity observation system is necessary in order to conduct field research on human activities. The authors have developed an ultrasonic 3D tag system, which is a type of location sensing system for observing human activities. The present study attempts to establish a systematic method for quickly constructing an ultrasonic 3D tag system in various environments. A calibration function that is available in various environments is one of the basic functions of portable ultrasonic 3D tag systems. In the present paper, we propose several methods for calibrating the 3D positions of ultrasonic receivers placed arbitrarily in a daily-use environment. The proposed methods require a relatively small number of transmitters and are independent of room size. In addition, the methods proposed herein are compared and their respective advantages are discussed. A portable system based on the proposed methods is also described herein.*

Keywords: Human Activity Observation, Ultrasonic Location Sensor, Calibration.

1 Introduction

Recently, human-centered information processing services have been attracting increasing attention. The goal of the present research is to establish a technique by which to recognize both human activity and state in a living space. Therefore, it is necessary to observe human activity in real time and with high-accuracy, without the presence of restraints that prevent natural human activities.

As a method for efficient and robust recognition of activities, the concept of object-based activity recognition has been proposed[7]. Theoretically, the behavior of handling objects in an environment such as an office or home can be recognized based on the motion of the objects. We have developed a three-dimensional (3D) ultrasonic location system as a fundamental system for robustly tracking objects and have verified that the observation of human activity based on object tracking is possible. However, like other location sensors, the developed ultrasonic location sensor has a disadvantage in that lack of portability makes it difficult to collect activity data in the various environments in which actual human activities occur.

In the present paper, we propose quick calibration algorithms that enable portable ultrasonic location sensors so that users can quickly construct a human activity observation system for field research on human activities.

2 Related Work

Several types of ultrasonic location systems have been proposed. The Bat Ultrasonic Location System [1, 2], developed by AT&T, and the MIT Cricket Indoor Location System [3] do not deal with a calibration method. The Novel Broadband Ultrasonic Location System [4] overcomes ultrasonic noise generated suddenly through everyday actions in a living space. This system takes the surrounding environment into consideration but does not deal with calibration. Although the DOLPHIN system [5] does not require calibration, this system is used only in narrow areas of approximately 2.5m × 2m, and the portability of the system is unknown. In addition, a calibration method using a robot [6] has been proposed, but the required calibration device is too large to use in a number of environments.

In contrast, the present study examines new calibration methods that require a relatively small number of transmitters and are independent of room size.

3 Quick Calibration

3.1 Calibration and measurement

The calibration herein describes the estimation of the 3D position of ultrasonic receivers required in order to measure the 3D positions of transmitters. Figure 1 shows the relation between the calibration and the measurement. In the measurement, transmitter positions are estimated from the known positions of receivers by solving an equation relating the transmitters and the receivers. In the calibration, receiver positions are calculated based on the known relative positions of transmitters. Both are essentially the same in the sense that unknown positions can be calculated based on known positions.

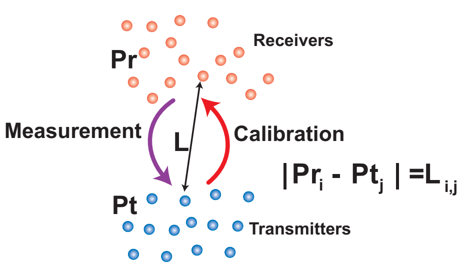

Figure 1: Calibration and measurement

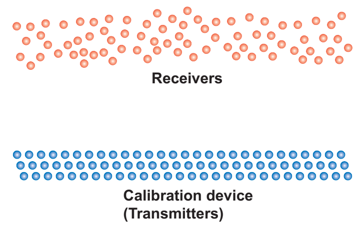

Figure 2: Typical calibration method 1

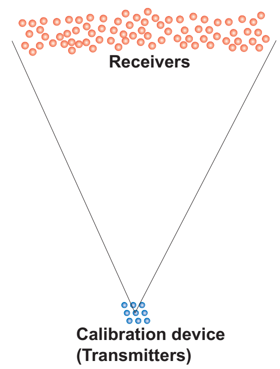

Figure 3: Typical calibration method 2

3.2 Simple calibration methods and disadvantages thereof

This section describes two typical calibration methods by directly applying a known estimation method of 3D positions.

3.2.1 Simple method 1: Large calibration device

The calibration device consists of transmitters of which the relative positions are known. This method involves the use of a calibration device of which the size is almost equal to the space containing the receivers, as shown in Fig. 2. However, fabricating, repositioning and using this large device is difficult.

3.2.2 Simple method 2: Small calibration device located at a distance from the receivers

This method involves placing a calibration device far away from receivers, the positions of which should be calibrated. This method cannot be used in enclosed spaces, such as spaces surrounded by walls and a ceiling.

3.3 Proposal of a quick calibration method

In the present paper, we propose two calibration methods in addition to two methods that can be used in conjunction with the basic methods described below.

3.3.1 Basic method 1: Three or more ultrasonic transmitters

The procedure for quick calibration method 1 is described below.

1. Move the calibration device arbitrarily to multiple positions (A, B, and C in Fig. 4).

2. Calculate the positions of receivers in a local coordinate system, with the local origin set at the position of the calibration system.

3. Select receivers for which the positions can be calculated from more than two calibration system positions.

4. Select a global coordinate system from among the local coordinate systems and calculate the positions of the calibration device in the global coordinate system using the receivers selected in Step 3. Then calculate transformation matrices ($\boldsymbol{M_1}$ and $\boldsymbol{M_2}$ in Fig. 4).

5. Calculate the receiver positions using the receiver positions calculated in Step 2 and the transformation matrices calculated in Step 4.

Steps 2 and 4 are described in detail in the following.

Calculating the 3D positions of receivers in a local coordinate system based on distance data (Step 2) The receiver position (x,y,z) is calculated by solving plane equations derived from the equations of intersecting spheres, as shown in Fig. 5, namely by the multilateration algorithm. This is explained in detail below.

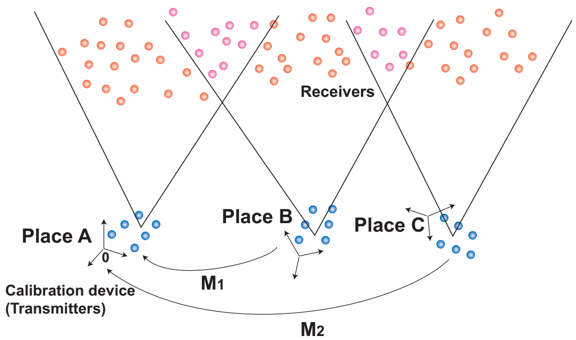

Figure 4: Quick calibration method 1

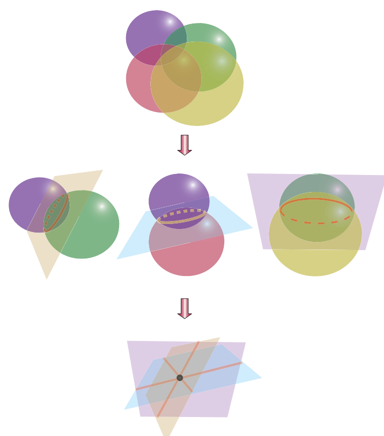

Figure 5: Multilateration

Here, $l_1, l_2, \cdots, l_i$ denote the distances from the ultrasonic receiver at (x,y,z) to the ith ultrasonic transmitter at position (x_i,y_i,z_i). We obtain the spherical equations as

$$\begin{aligned}
(x_1 - x)^2 + \quad (y_1 - y)^2 \quad + (z_1 - z)^2 &= l_1^2, && (1)\\
(x_2 - x)^2 + \quad (y_2 - y)^2 \quad + (z_2 - z)^2 &= l_2^2, && (2)\\
(x_3 - x)^2 + \quad (y_3 - y)^2 \quad + (z_3 - z)^2 &= l_3^2, && (3)\\
&\vdots \\
(x_i - x)^2 + \quad (y_i - y)^2 \quad + (z_i - z)^2 &= l_i^2. && (4)
\end{aligned}$$

We obtain equations for the intersecting planes between the spheres from (1), (2), (3) and (4) as

$$\begin{aligned}
& 2\,(x_2 - x_1)\,x + 2\,(y_2 - y_1)\,y + 2\,(z_2 - z_1)\,z \\
= \;& l_1^2 - x_1^2 - y_1^2 - z_1^2 - l_2^2 + x_2^2 + y_2^2 + z_2^2, && (5)\\
& 2\,(x_3 - x_1)\,x + 2\,(y_3 - y_1)\,y + 2\,(z_3 - z_1)\,z \\
= \;& l_1^2 - x_1^2 - y_1^2 - z_1^2 - l_3^2 + x_3^2 + y_3^2 + z_3^2, && (6)\\
& \vdots \\
& 2\,(x_i - x_1)\,x + 2\,(y_i - y_1)\,y + 2\,(z_i - z_1)\,z \\
= \;& l_1^2 - x_1^2 - y_1^2 - z_1^2 - l_i^2 + x_i^2 + y_i^2 + z_i^2. && (7)
\end{aligned}$$

Simultaneous linear equations are obtained from the above equations as

$$\mathbf{AP} = \mathbf{B}, \qquad (8)$$

$$\text{where} \quad \mathbf{P} = \begin{pmatrix} x \\ y \\ z \end{pmatrix}, \qquad (9)$$

$$\mathbf{A} = \begin{pmatrix} 2(x_2 - x_1) & 2(y_2 - y_1) & 2(z_2 - z_1) \\ 2(x_3 - x_1) & 2(y_3 - y_1) & 2(z_3 - z_1) \\ \vdots & \vdots & \vdots \\ 2(x_i - x_1) & 2(y_i - y_1) & 2(z_i - z_1) \end{pmatrix}, \qquad (10)$$

$$\mathbf{B} = \begin{pmatrix} l_1^2 - x_1^2 - y_1^2 - z_1^2 - l_2^2 + x_2^2 + y_2^2 + z_2^2 \\ l_1^2 - x_1^2 - y_1^2 - z_1^2 - l_3^2 + x_3^2 + y_3^2 + z_3^2 \\ \vdots \\ l_1^2 - x_1^2 - y_1^2 - z_1^2 - l_i^2 + x_i^2 + y_i^2 + z_i^2 \end{pmatrix}. \qquad (11)$$

For the case of four or more transmitters that are not coplanar, the rank of $\mathbf{A}$ becomes 3. The position (x,y,z) can be calculated by the least squares method as

$$\mathbf{P} = (\mathbf{A^T A})^{-1} \mathbf{A^T B}. \qquad (12)$$

Reference [7] presents a detailed description for the case in which the rank of $\mathbf{A}$ is 2.

Calculating the positions of the calibration device in the global coordinate system (Step 4) Here, let us assume that the calibration device has n transmitters, that m receivers are to be calibrated, and that the user repositions the device at four different positions (positions A, B, C, and D) for calibration.

In the local coordinate system having the origin at A (position A), the calculated receiver positions are denoted by $(x_{r_A1}, y_{r_A1}, z_{r_A1})$, $(x_{r_A2}, y_{r_A2}, z_{r_A2})$, $\cdots$, $(x_{r_Ai_A}, y_{r_Ai_A}, z_{r_Ai_A})$ and the transmitter positions are $(x_{t_A1}, y_{t_A1}, z_{t_A1})$, $(x_{t_A2}, y_{t_A2}, z_{t_A2})$, $\cdots$, $(x_{t_An}, y_{t_An}, z_{t_An})$, where i_A indicates the number of receivers calculated from position A. Generally, i_A is smaller than m because of the directivity of the transmitters. The corresponding transmitter positions in the global coordinate system are denoted by $(X_{t_A1}, Y_{t_A1}, Z_{t_A1})$, $(X_{t_A2}, Y_{t_A2}, Z_{t_A2})$, $\cdots$, $(X_{t_An}, Y_{t_An}, Z_{t_An})$.

Similarly, in the local coordinate system having the origin at B (position B), the calculated receiver positions are denoted by $(x_{r_B1}, y_{r_B1}, z_{r_B1})$,$(x_{r_B2}, y_{r_B2}, z_{r_B2})$, $\cdots$, $(x_{r_Bi_B}, y_{r_Bi_B}, z_{r_Bi_B})$ and the transmitter positions are $(x_{t_B1}, y_{t_B1}, z_{t_B1})$, $(x_{t_B2}, y_{t_B2}, z_{t_B2})$, $\cdots$, $(x_{t_Bn}, y_{t_Bn}, z_{t_Bn})$. In the global coordinate system, the transmitter positions are denoted by $(X_{t_B1}, Y_{t_B1}, Z_{t_B1})$, $(X_{t_B2}, Y_{t_B2}, Z_{t_B2})$, $\cdots$, $(X_{t_Bn}, Y_{t_Bn}, Z_{t_Bn})$.

There are receivers (pink spheres in Fig. 4) of which the positions can be calculated from both positions A and B. For example, if $(x_{r_A10}, y_{r_A10}, z_{r_A10})$, $(x_{r_A11}, y_{r_A11}, z_{r_A11})$,

$\cdots$, $(x_{rA}18, y_{rA}18, z_{rA}18)$ are the positions in local coordinate system A, and $x_{rB}9, y_{rB}9, z_{rB}9)$, $(x_{rB}10, y_{rB}10, z_{rB}10)$, $\cdots$, $(x_{rB}18, y_{rB}18, z_{rB}18)$ are the corresponding positions in local coordinate system B, then we can obtain the following equation:

$$\mathbf{P_A} = \mathbf{M_{BA}} \mathbf{P_B}, \tag{13}$$

$$\tag{14}$$

where $\mathbf{M_{BA}}$ is a 4×4 matrix, and

$$\mathbf{P_A} = \begin{pmatrix} x_{rA}10 & x_{rA}11 & \cdots & x_{rA}18 \\ y_{rA}10 & y_{rA}11 & \cdots & y_{rA}18 \\ z_{rA}10 & z_{rA}11 & \cdots & z_{rA}18 \\ 1 & 1 & \cdots & 1 \end{pmatrix}, \tag{15}$$

$$\mathbf{P_B} = \begin{pmatrix} x_{rB}1 & x_{rB}2 & \cdots & x_{rB}9 \\ y_{rB}1 & y_{rB}2 & \cdots & y_{rB}9 \\ z_{rB}1 & z_{rB}2 & \cdots & z_{rB}9 \\ 1 & 1 & \cdots & 1 \end{pmatrix}. \tag{16}$$

The matrix $\mathbf{M_{BA}}$ can be calculated by the least squares method as follows:

$$\mathbf{M_{BA}} = \mathbf{P_A} \mathbf{P_B^T} (\mathbf{P_B} \mathbf{P_B^T})^{-1} \tag{17}$$

The transformation matrix $\mathbf{M_{BA}}$ in (17) has effects of not only rotation and translation but also enlargement and reduction. This matrix distorts the coordinate system for the case in which the transformation of the coordinate system is performed using multiple matrices, as described later. We use the matrix expressed by

$$\begin{pmatrix} \cos\alpha\cos\beta\cos\gamma - \sin\alpha\sin\gamma & -\sin\alpha\cos\gamma - \cos\alpha\cos\beta\sin\gamma & \cos\alpha\sin\beta & \mathrm{Tx} \\ \sin\alpha\cos\beta\cos\gamma - \cos\alpha\sin\gamma & \cos\alpha\cos\gamma - \sin\alpha\cos\beta\sin\gamma & \sin\alpha\sin\beta & \mathrm{Ty} \\ -\sin\beta\cos\lambda & \sin\beta\sin\gamma & \cos\beta & \mathrm{Tz} \\ 0 & 0 & 0 & 1 \end{pmatrix}, \tag{18}$$

where α is the angle of rotation about the z-axis, β is the angle of rotation about the new y-axis, γ is the angle of rotation about the new z-axis, and the matrix is translated by Tx, Ty, and Tz. We can calculate $\alpha, \beta, \gamma, Tx, Ty$, and Tz using a non-linear optimization method, such as the Nelder-Mead downhill simplex method.

The receiver positions $\mathbf{P_B}$ in the local coordinate system based on position B can be converted to the positions $\mathbf{P_B^w}$ in the global coordinate system (or in the local coordinate system based on position A) as follows:

$$\mathbf{P_B^w} = \mathbf{M_{ba}} \cdot \mathbf{P_B}. \tag{19}$$

Similarly, we can also calculate $\mathbf{M_{BA}}, \mathbf{M_{CB}}$, and $\mathbf{M_{DC}}$.

$$\mathbf{P_C^w} = \mathbf{M_{BA}} \cdot \mathbf{M_{CB}} \cdot \mathbf{P_C}, \tag{20}$$

$$\mathbf{P_D^w} = \mathbf{M_{BA}} \cdot \mathbf{M_{CB}} \cdot \mathbf{M_{DC}} \cdot \mathbf{P_D}. \tag{21}$$

In this way, we can calculate all of the receiver positions in the global coordinate system.

3.3.2 Basic method 2: Ultrasonic transmitter

The procedure for quick calibration method 2 is described below.

1. Determine the positions of three ultrasonic receivers by measuring L_1, L_2 and L_3 among the three receivers selected arbitrarily.
2. Calculate each of the positions of an arbitrarily positioned transmitter from the three receiver positions calculated in Step 2.
3. In a similar way, calculate the 3D positions of the receivers by selecting four or more such arbitrary transmitter positions.

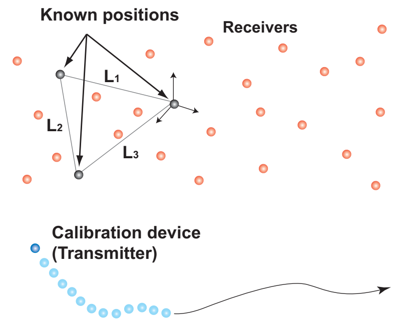

Figure 6: Quick calibration method 2

3.3.3 Additional method 1: Coplanar constraint

The calibration error can be improved significantly based on knowledge of configuration of the receivers to be calibrated. For example, by placing the ultrasonic receivers on the ceiling or on a wall, we can take advantage of the fact that the receivers are located on the same plane. This section describes a method for calibrating the positions of receivers when the receivers are located on the same plane.

Figure 7 shows the coplanar constraint method. $\mathbf{Pr}_i$ (= (x_i, y_i, z_i)) denotes the positions of receivers, $\mathbf{Pt}_j$ denotes the positions of transmitters, and $\mathbf{n}$ denotes the normal vector to the plane.

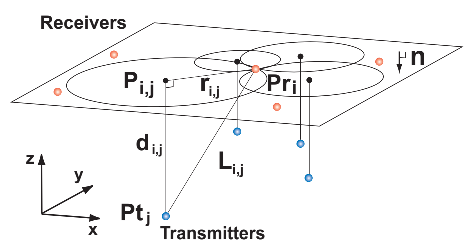

Figure 7: Coplanar constraint

The equation for the plane on which all of the receivers are located can be written as

$$ax + by + cz + d = 0. \tag{22}$$

We can calculate the optimal values of these variables (a, b, c, d) in the least squares sense using (23). Concretely, these variables (a, b, c, d) can be calculated as a basic vector of nullspace by performing singular value decomposition.

$$\begin{pmatrix} x_1 & y_1 & z_1 & 1 \\ x_2 & y_2 & z_2 & 1 \\ \vdots & \vdots & \vdots & \vdots \\ x_i & y_i & z_i & 1 \end{pmatrix} \begin{pmatrix} a \\ b \\ c \\ d \end{pmatrix} = 0, \tag{23}$$

where (x_i, y_i, z_i) are temporary solutions for receivers as calculated by basic method 1 or basic method 2.

If perpendiculars are dropped from the transmitters, we can calculate the intersection points of the plane and the perpendiculars denoted by $\mathbf{P}_{i,j}(= (x_{i,j}, y_{i,j}, z_{i,j}))$. We can then calculate the distance $d_{i,j}$ and the length $r_{i,j}$.

The positions of the receivers are $\mathbf{Pr}_i$, and the equations of spheres centered at $\mathbf{P}_{i,j}$ with radii $r_{i,j}$ are

$$(x_{i,1} - x_i)^2 + (y_{i,1} - y_i)^2 + (z_{i,1} - z_i)^2 = r_{i,1}, \tag{24}$$
$$(x_{i,2} - x_i)^2 + (y_{i,2} - y_i)^2 + (z_{i,2} - z_i)^2 = r_{i,2}, \tag{25}$$
$$\vdots$$
$$(x_{i,j} - x_i)^2 + (y_{i,j} - y_i)^2 + (z_{i,j} - z_i)^2 = r_{i,j}. \tag{26}$$

The positions of receivers are located on the intersection points of these spheres. The plane equations derived from these spheres are expressed as follows:

$$\mathbf{APr}_i = \mathbf{B}, \tag{27}$$

$$\text{where} \quad \mathbf{Pr}_i = \begin{pmatrix} x_i \\ y_i \\ z_i \end{pmatrix}, \tag{28}$$

$$\mathbf{A} = \begin{pmatrix} 2(x_{i,2} - x_{i,1}) & 2(y_{i,2} - y_{i,1}) & 2(z_{i,2} - z_{i,1}) \\ 2(x_{i,3} - x_{i,1}) & 2(y_{i,3} - y_{i,1}) & 2(z_{i,3} - z_{i,1}) \\ 2(x_{i,4} - x_{i,1}) & 2(y_{i,4} - y_{i,1}) & 2(z_{i,4} - z_{i,1}) \\ \vdots & \vdots & \vdots \end{pmatrix}, \tag{29}$$

$$\text{and} \quad \mathbf{B} = \begin{pmatrix} r_{i,1}^2 - x_{i,1}^2 - y_{i,1}^2 - z_{i,1}^2 - r_{i,2}^2 + x_{i,2}^2 + y_{i,2}^2 + z_{i,2}^2 \\ r_{i,1}^2 - x_{i,1}^2 - y_{i,1}^2 - z_{i,1}^2 - r_{i,3}^2 + x_{i,3}^2 + y_{i,3}^2 + z_{i,3}^2 \\ r_{i,1}^2 - x_{i,1}^2 - y_{i,1}^2 - z_{i,1}^2 - r_{i,4}^2 + x_{i,4}^2 + y_{i,4}^2 + z_{i,4}^2 \\ \vdots \end{pmatrix}. \tag{30}$$

The rank of $\mathbf{A}$ is always 2 because of the coplanar constraint. We calculate $\mathbf{Pr}_i$ using (22), and (31) $\sim$ (33).

$$\mathbf{Pr}_i = \mathbf{Pr}_{i0} + \mathbf{n} \cdot t, \tag{31}$$
$$\mathbf{Pr}_{i0} = \mathbf{A}^+\mathbf{B}, \tag{32}$$
$$\mathbf{n} = (\mathbf{a}, \mathbf{b}, \mathbf{c}) \tag{33}$$

where $\mathbf{A}^+$ indicates the Moore-Penrose inverse matrix of $\mathbf{A}$.

3.3.4 Additional method 2: Consideration of directivities

Error due to ultrasonic damping

The authors discovered a phenomenon whereby the measured distance between receivers and transmitters is longer than actual distance due to ultrasonic damping. This phenomenon causes an increase in the error. The damping is caused by the directivities of the transmitter and the receiver. This section describes a method that considers the directivities in order to reduce this effect.

The ultrasonic location system developed by our group measures the distance from the time-of-flight of the ultrasonic pulse. The time at which the ultrasonic wave exceeds the threshold is the arrival time of the ultrasonic pulse at the receiver, as shown in Fig. 8. However, in the case of damping of the ultrasonic wave, due to the effects of directivity and distance, the error of the measured distance increases as a result of the delay in the ultrasonic pulse arrival time expressed by ΔT.

Approach to the damping problem

There are two approaches to this problem; a hardware approach and a software approach. In the hardware approach, for example, the highest point of the ultrasonic wave can be assumed to be the ultrasonic pulse arrival time determined by sampling and analyzing the ultrasonic wave, which requires expensive equipment. Therefore, in the present paper, we describe the software approach.

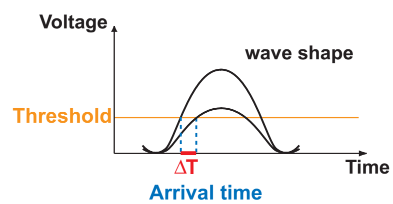

Figure 8: Measurement of ultrasonic pulse arrival time

Method for dealing with the damping problem

The distance between the receivers and transmitters is

$$|\mathbf{Pr}_i - \mathbf{Pt}_j| = L_{ij}, \tag{34}$$

where $\mathbf{Pr}_i$ are the positions of the receivers, $\mathbf{Pt}_j$ are the positions of the transmitters, and L_{ij} are the actual distances. The distances $L_{m,ij}$ measured ultrasonically are longer than the actual distances L_{ij}. The actual distances L_{ij} are described by

$$L_{ij} = L_{m,ij} - \Delta L_{ij}, \tag{35}$$

where ΔL_{ij} is the error of the distance.

The direction of the transmitting face is denoted by $\mathbf{z}$ and the direction of the receiving face is denoted by $\mathbf{n}$. Then

$$\cos\theta_{ij} = \frac{(\mathbf{Pr}_i - \mathbf{Pt}_j) \cdot \mathbf{z}}{|\mathbf{Pr}_i - \mathbf{Pt}_j| \cdot |\mathbf{z}|}, \tag{36}$$

$$\cos\phi_{ij} = \frac{(\mathbf{Pt}_j - \mathbf{Pr}_i) \cdot \mathbf{n}}{|\mathbf{Pt}_j - \mathbf{Pr}_i| \cdot |\mathbf{n}|}. \tag{37}$$

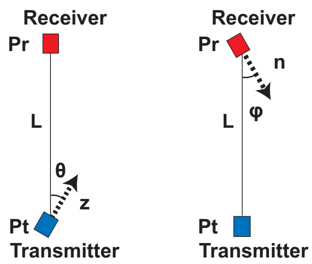

Figure 9: Angle and distance

In this case all of the directions of transmitters are identical, as are all of the directions of the receivers. Actually it is easy to create the calibration device in which the transmitters are attached in the same direction. In addition, setting the receivers in the same direction is easy.

The experimentally obtained relationship between the transmitting angle of a transmitter and the error and that between the receiving angle of a receiver and the error are shown in Figure 10 and Figure 11, respectively.

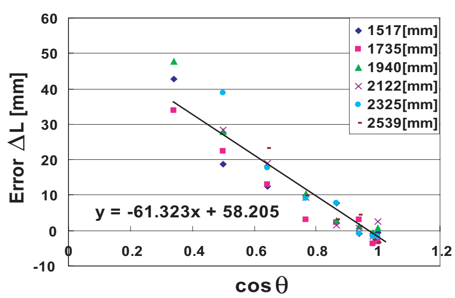

Figure 10: Relationship between transmitting angle and error

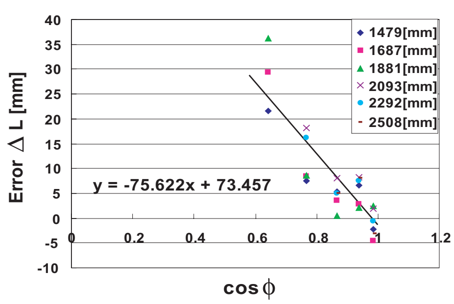

Figure 11: Relationship between receiving angle and error

Here,

$$\Delta L_{ij} = -61.323 \cos\theta_{ij} - 75.622 \cos\phi_{ij} + 131.662 \quad (38)$$

was obtained experimentally.

In the equation

$$E = \sum_{i,j} \left(|\mathbf{Pt}_j - \mathbf{Pr}_i|^2 - L_{ij}^2 \right)^2, \quad (39)$$

the receiver positions $\mathbf{Pr}_i$ are calculated by minimizing E using a non-linear optimization method (such as the Nelder-Mead downhill simplex method).

4 Experiments

4.1 System configuration

Figure 12 shows the system configuration for the proposed 3D ultrasonic tag system. The system consists of an ultrasonic receiving section, an ultrasonic transmitting section, a time-of-flight measurement section, a network section, and a personal computer. The ultrasonic receiving section receives ultrasonic pulses emitted from the ultrasonic transmitter and amplifies the received signal. The time-of-flight measurement section records the travel time of the signal from transmission to reception. The network section synchronizes the system and collects time-of-flight data from the ultrasonic receiving section. The positions of objects are calculated based on more than three time-of-flight results.

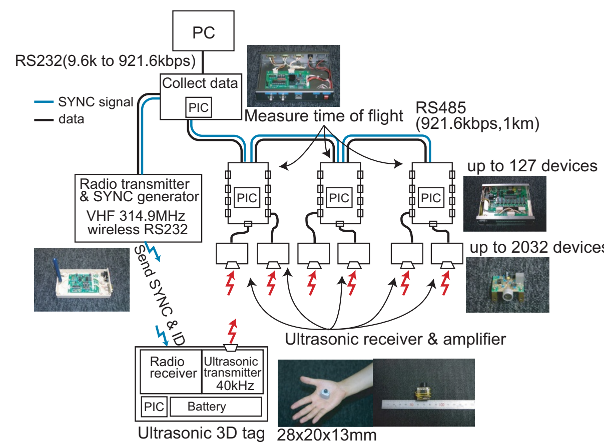

Figure 12: System configuration

4.2 Experimental results

4.2.1 Method for error evaluation

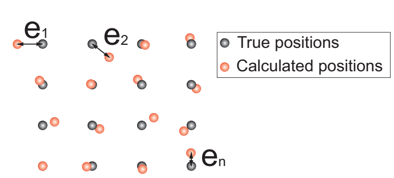

Figure 13: Method for calculating error

Figure 13 shows the method used to calculate error. The distances between the calculated receiver positions and the true receiver positions are denoted by $e_1, e_2, \cdots, e_n$. The average error is defined by

$$E = \frac{1}{n} \sum_{i=1}^{n} e_i. \quad (40)$$

4.2.2 Accuracy evaluation

Calibration was performed in a room (4.0×4.0×2.5 m) having 120 ultrasonic receivers embedded in the ceiling. Figure 14 shows the experimental results of proposed calibration method 1 applied using the coplanar constraint. The authors performed calibration at 16 points in the room. Seventy-six receivers were calculated. In the figure, the red spheres indicate calculated receiver positions, whereas the black crosses are the true receiver positions, and the blue spheres indicate the positions of the calibration device. Figure 15 shows the experimental results for proposed calibration method 1 considering directivities. Seventy-six receivers were calculated. Figure 16 shows the experimental results of proposed calibration method 2 using the coplanar constraint. Seventy-six receivers were calculated. Table 1 shows the average error E, maximum error, and minimum error for these methods.

The transmitter position error was 40 to 320 mm in the case of calibration based on basic method 1 considering directivities.

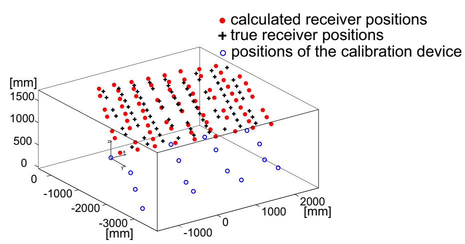

Figure 14: Experimental results for proposed method 1 with the coplanar constraint

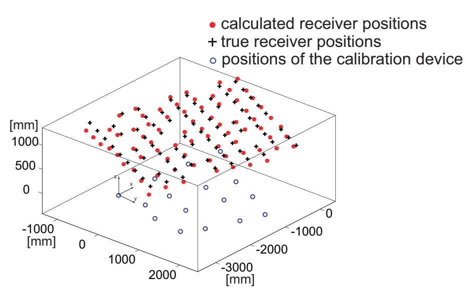

Figure 15: Experimental results for proposed method 1 considering directivity

5 Advantages of the Proposed Methods

The advantages and disadvantages of the proposed calibration methods are listed below.

Basic method 1: Three or more ultrasonic transmitters
advantage: Suitable for wide-area calibration.
disadvantage: Requires a calibration device.
Basic method 2: Ultrasonic transmitter
advantage: Easy to use because only a single transmitter is needed.

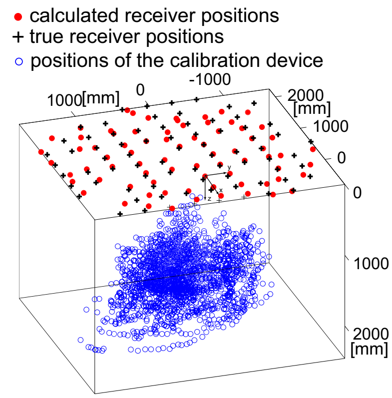

Figure 16: Experimental results for proposed method 2 with the coplanar constraint

Table 1: Errors in the proposed methods

	Average error	Maximum error	Minimum error
Method 1	195 mm	399 mm	66 mm
Method 1 with coplanar constraint	186 mm	382 mm	26 mm
Method 1 considering directivity	78 mm	341 mm	13 mm
Method 1 considering directivity with coplanar constraint	74 mm	338 mm	11 mm
Method 2	239 mm	3000 mm	27 mm
Method 2 with coplanar constraint	112 mm	542 mm	2 mm
Method 2 considering directivity	impossible	impossible	impossible
Method 2 considering directivity with coplanar constraint	impossible	impossible	impossible

disadvantage: Not suitable for wide-area calibration.
Additional method 1: Coplanar constraint
advantage: Improved accuracy.
disadvantage: Only applicable in the coplanar case.
Additional method 2: Consideration of directivities
advantage: Improved accuracy.
disadvantage: Calculation requires a great deal of time. The directions of the receivers are assumed to be identical.

6 Realized Ultrasonic Portable 3D Tag System

The proposed methods enable a portable ultrasonic 3D tag system. Figure 17 shows a portable ultrasonic 3D tag system, which consists of a case, tags, receivers, and a calibration device. The portable system enables measurement of human activities by quickly installing and calibrating the system on-site, at the location where the activities actually occur.

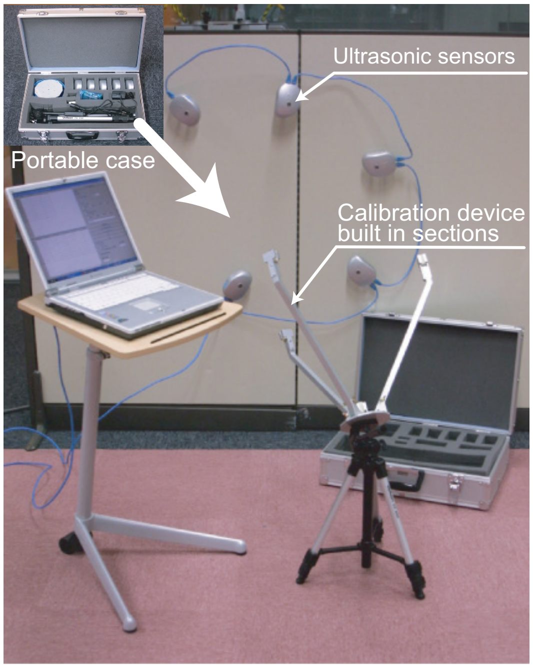

Figure 17: Realized portable ultrasonic 3D tag system

7 Conclusion

In the present paper, we proposed new calibration methods to enable a portable ultrasonic location sensor so that users can quickly construct a system for observing human activity in various environments where human activities actually occur. Two basic calibration methods and two additional methods for quick calibration were described: B1) a basic method using three or more transmitters, B2) a basic method using a single transmitter, A1) an additional method using the coplanar constraint, and A2) an additional method considering the directivities of ultrasonic transmitters and receivers. One of the advantages of all of the proposed methods is the requirement for a relatively small number of transmitters. In addition, the proposed methods are not dependent on room size.

The performance of the proposed methods was tested in an experimental room (4.0×4.0×2.7m) in which 120 ultrasonic receivers were attached to the ceiling. The experimental results showed that the proposed methods could be used to calibrate the positions of receivers positioned over a space larger than that of the calibration device and that the error of calibration could be improved significantly by considering coplanar constraints or ultrasonic directivity. In the case of calibration using four transmitters with the coplanar constraint and considering directivities, the average of position error was 76 mm, a 60% decrease compared to the case without the coplanar constraint or consideration of directivities. The advantages and disadvantages of the proposed methods were discussed herein.

In addition, a portable ultrasonic location sensor based on the proposed methods was realized. The portable system allows human activities to be measured in the area where the activities actually occur with quick installation and calibration.

Further studies will examine the refinement of the method in order to measure the 3D positions with higher accuracy, systematization of calibration methods, and the use of the portable 3D ultrasonic tag system in a living space.

Acknowledgment

This study was funded in part by a Grant-in-Aid as part of the Special Coordination Fund for Promoting Science and Technology from the Ministry of Education, Culture, Sports, Science and Technology of Japan.

References

[1] Andy Ward, Alan Jones, and Andy Hopper, "A New Location Technique for the Active Office," *IEEE Personal Communications*, Vol.4, No.5, pp. 42-47, October 1997.

[2] Mike Addlesee, Rupert Curwen, Steve Hodges, Joe Newman, Pete Steggles, Andy Ward, and Andy Hopper, "Implementing a sentient computing system," *IEEE Computer*, Vol.34, No.8, pp. 50-56, August 2001.

[3] Nissanka B. Priyantha, Anit Chakraborty, and Hari Balakrishnan, "The Cricket Location-Support system," *in Proceedings of the 6th International Conference on Mobile Computing and Networking (ACM MobiCom2000)*, August 2000.

[4] Mike Hazas and Andy Ward, "A Novel Broadband Ultrasonic Location System," *in Proceedings of UbiComp 2002*, September 2002.

[5] Y. Fukuju, M. Minami, H. Morikawa, and T. Aoyama, "DOLPHIN: An Autonomous Indoor Positioning System in Ubiquitous Computing Environment," *in Proceedings of IEEE Workshop on Software Technologies for Future Embedded Systems (WSTFES2003)*, pp. 53-56, May 2003.

[6] A. Mahajan and F. Figueroa, "An Automatic Self Installation and Calibration Method for a 3D Position Sensing System using Ultrasonics," *Robotics and Autonomous Systems*, Vol. 28, No. 4, pp. 281-294, September 1999.

[7] Y. Nishida, H. Aizawa, T. Hori, N.H. Hoffman, T. Kanade, and M. Kakikura, "3D Ultrasonic Tagging System for Observing Human Activity," *in Proceedings of IEEE International Conference on Intelligent Robots and Systems (IROS2003)*, pp. 785-791, October 2003.